Journal of Structural Geology, Vol. 7, No. 1, pp. 19 to 35, 1985
Printed in Great Britain.

0191-8141/85 $03.00 + 0.00

Structural history of high-pressure metamorphic rocks in the southern Vanoise massif, French Alps, and their relation to Alpine tectonic events

J. P. PLATT

Department of Geology and Mineralogy, University of Oxford, Parks Road, Oxford OX1 3PR, U.K.

and

G. S. LISTER*

Department of Structural Geology, Institute for Earth Sciences, University of Utrecht, The Netherlands

(*Received* 31 *October* 1983; *accepted in revised form* 23 *March* 1984)

Abstract—A nappe of amphibolite-facies metamorphic rocks of pre-Permian age in the southern Vanoise massif (the Arpont schist) has been affected by an Alpine HP/LT metamorphism. The first mesoscopically recognizable deformation (D_1) post-dated the high-pressure peak (jadeitic pyroxene + quartz, glaucophane + ?lawsonite), and was associated with glaucophane + epidote. D_1 produced a flat-lying schistosity and a NW-trending glaucophane lineation, and was probably associated with nappe displacement involving NW-directed subhorizontal shear. D_2 formed small-scale folds and a foliation associated with chlorite + albite. The changing parageneses during the period pre-D_1 to D_1 to D_2 suggest decreasing pressure, so that the deformation appears to have been related to the uplift history, rather than to the process of tectonic burial. D_2 was followed by a static metamorphism (green biotite + chlorite + albite), possibly of Lepontine age. SE-directed backthrusting and folding (D_3), and later differential uplift along steep faults, took place under low-grade conditions.

INTRODUCTION

THE VANOISE massif is a terrain consisting of pre-Permian schists and pre-Triassic to Eocene low-grade metasedimentary rocks. High-pressure/low-temperature metamorphic mineral assemblages of Alpine age are locally developed in the pre-Permian rocks. The terrain forms part of the Penninic allochthon of the Western Alps (Fig. 1), and in a broad sense is a southern continuation of the Grand Saint Bernard nappe of the Swiss Alps. In palaeogeographic terms it is regarded as part of the Briançonnais platform, on the basis of the thin and incomplete stratigraphy of the Mesozoic sequence (Ellenberger 1958, Debelmas 1974). The terrain is regionally overlain by rocks of the Piémont zone, comprising nappes of metamorphosed calcareous sediments (Schistes lustrés) and ophiolitic rocks from the margins of the Piémont oceanic basin. On the west side it is juxtaposed along a zone of steep faults with the Zone Houillère: a belt of low-grade Permian and Carboniferous metasediments (Fig. 2).

The Pennine Zone as a whole is a composite tectonic assemblage formed during subduction and closure of the Piémont ocean in late Cretaceous–Eocene time (Trümpy 1975, Milnes 1978, Homewood *et al.* 1979), and it was emplaced as a major allochthon onto the European continental margin in Oligocene time (Frisch 1979). Large areas of the Pennine Zone show the so-called "Eo-Alpine" high-pressure/low-temperature metamorphism, caused by rapid tectonic burial during subduction and collision (Ernst 1973, Frey *et al.* 1974, Desmons 1977). Isotopic dating of the Eo-Alpine metamorphism in the structurally highest units of the Western Alps (the Sesia Zone, the Monte Rosa nappe, and the Zermatt–Saas ophiolites) show that subduction and metamorphism of these units occurred in Late Cretaceous time, roughly between 110 and 70 Ma ago (Frey *et al.* 1976, Bocquet *et al.* 1974, Delaloye & Desmons 1976). This predated the final closure of the Piémont ocean, suggesting that these terrains lay within the oceanic domain. Their emplacement into their present tectonic positions occurred during the meso-Alpine tectonic event in Eocene time, and post-dated the Eo-Alpine high P/T metamorphism, as the presently observed nappe contacts juxtapose rocks with different metamorphic assemblages (Compagnoni *et al.* 1976, Desmons 1977). The Briançonnais platform (including the Vanoise), on the other hand, probably lay close to the edge of the southern European continental margin, from which it was separated by the Valais and sub-Briançonnais troughs. High P/T metamorphism in this area may therefore have been later than in the high Penninic units, and may have been directly related to final closure of the Piémont ocean and the construction of the present pile of Pennine nappes. Unfortunately, K/Ar dating of the high P/T metamorphism in the Vanoise has been hindered by inherited argon in pre-Permian rocks (Bocquet *et al.* 1974).

Our aim in studying the high-pressure rocks of the Vanoise massif was to help constrain models for this part of the Alpine orogen by relating the metamorphic history in detail to the tectonic development of the area. We were particularly interested to see if the deep tec-

*Present address: Bureau of Mineral Resources, P.O. Box 378, Canberra City, Australia.

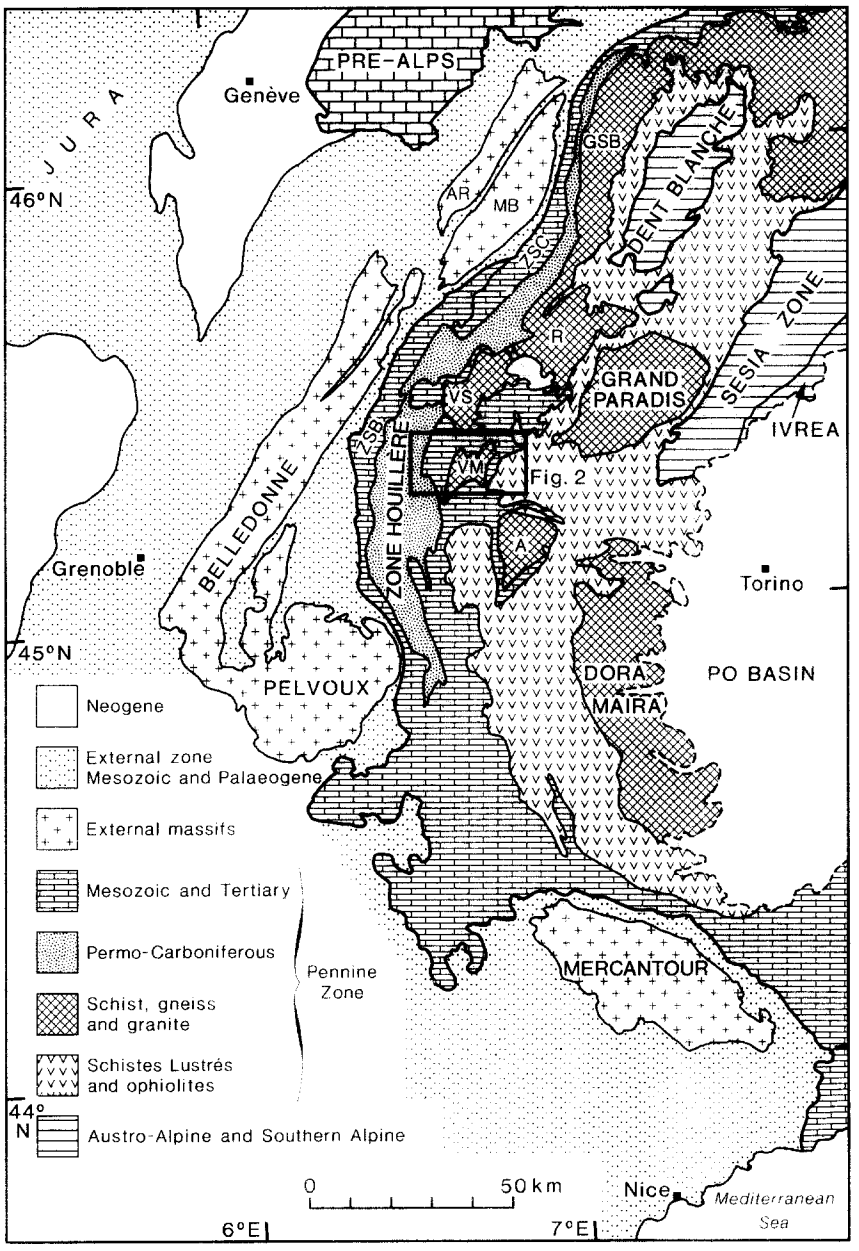

Fig. 1. Tectonic sketch map of the western Alps. Abbreviations: External massifs: AR, Aiguilles Rouges; MB, Mont Blanc. Pennine Front: ZSC, Zone Sion-Courmayeur; ZSB, Zone Sub-Briançonnais. Schist and gneiss massifs of the Grand Saint Bernard Group: GSB, Grand Saint Bernard; R, Ruitor; Vanoise Septentrional (northern Vanoise); VM, Vanoise Meridional (southern Vanoise); A, Ambin.

tonic burial required for high-pressure metamorphism, and the subsequent uplift required for preservation of the mineral assemblages and exposure of the rocks at their present level, were recorded in the form of large-scale structures or penetrative deformation.

TECTONIC SETTING

The principal occurrence of high-pressure rocks in the Vanoise massif is a body of metasedimentary and metabasic rocks referred to here as the Arpont schist. This has traditionally been treated as part of a pre-Permian "basement" to the Permian-Eocene "cover" in the area (Ellenberger 1958, Raoult 1980). There is evidence for four metamorphic events in the Arpont schist (Bocquet 1971, 1974a, b, Bocquet *et al.* 1974): (a) a pre-Permian amphibolite-facies metamorphism; (b) a Permian thermal event, possibly related to the intrusion of acid magmas; (c) a relatively early Alpine high-pressure metamorphism, and (d) partial alteration of the earlier assemblages under greenschist-facies conditions.

Over much of its outcrop area the Arpont schist is overlain by inverted Mesozoic rocks (Figs. 3 and 4), so that its upper boundary is tectonic (Platt & Lister 1978). A lower boundary has not previously been recognized, but we believe that it is exposed where the entire tectonic sequence in the area has been turned up on end by late backfolding (Fig. 3). Before backfolding it appears that the Arpont schist overlay an inverted sequence of pre-Triassic metaclastic rocks that have a non-conformable boundary with the schist. We therefore argue that the

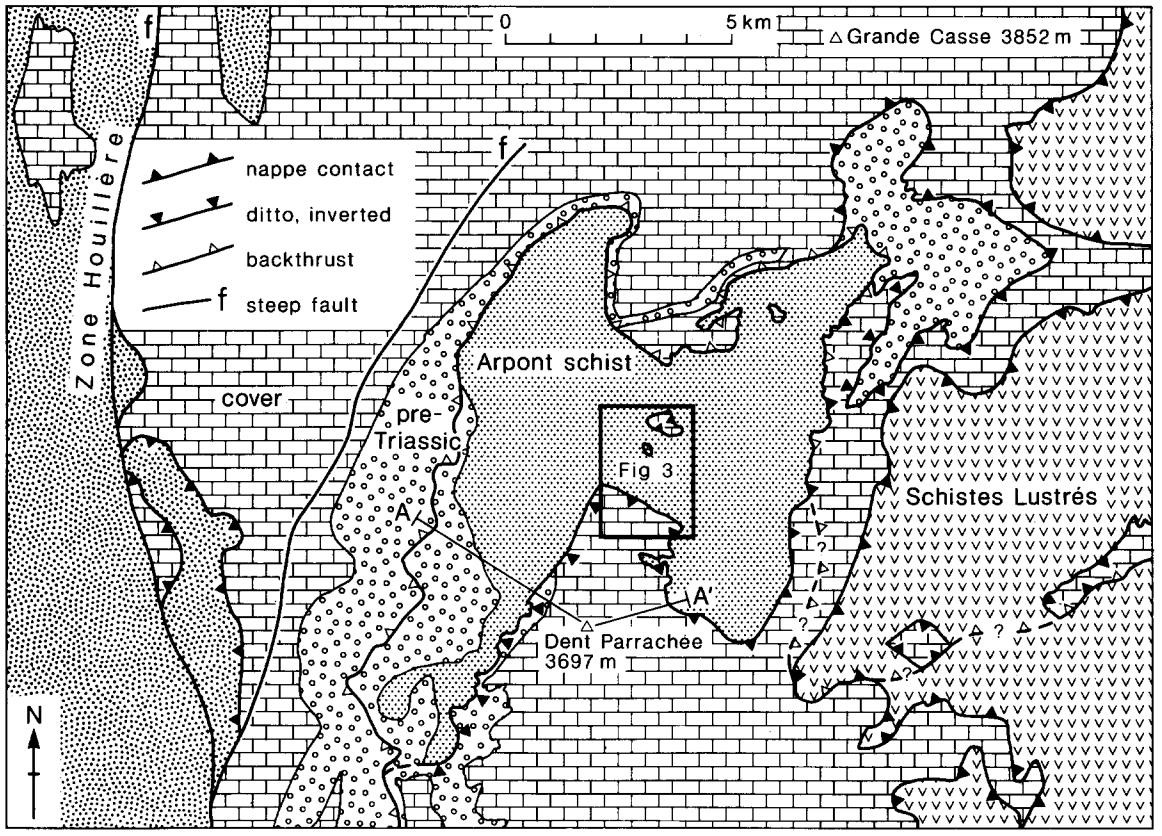

Fig. 2. Geological setting of the southern Vanoise massif. See Fig. 1 for location. Based on mapping by the authors and students of the Universities of Oxford and Utrecht, and on the Annecy 1:250,000 geological map sheet (BRGM 1979). *Pre-Triassic:* greenschist-facies metasediments of probable Permian age. *Cover:* Triassic to Eocene.

Arpont schist forms a sheet-like tectonic unit involving a disrupted recumbent fold. Such a structure can best be described as a nappe.

There has been some debate as to whether the Arpont schist has experienced the same metamorphic history as the rest of the Vanoise. Bocquet (Desmons) (1974, 1977) documented the assemblage jadeite + quartz from the Arpont schist, and estimated a peak pressure of over 10 kb at a temperature of not more than 350°C. She therefore suggested that the Arpont schist may have experienced a more extreme and possibly earlier HP/LT metamorphism than the surrounding rocks, which lack jadeite or glaucophane. The significance of the jadeite + quartz assemblage was challenged by Saliot (1979) and Goffé (1982), and the latter estimated peak conditions in both the Arpont schist and the Permian–Eocene cover of the area at 6–7 kb and 300–350°C, based on the association of Fe,Mg-carpholite + chloritoid + lawsonite + quartz in metabauxite. We discuss the significance of our observations to this debate in a later section.

ROCK TYPES AND PETROGRAPHY

Arpont schist

The Arpont schist includes a variety of rock-types resulting partly from differences in primary composition and texture, and partly from the variable impact of several metamorphic and deformational events.

(i) *Grey quartz–mica–schist.* This is by far the most abundant rock-type. It is presumably derived from a quartz-rich clastic sediment, but we have found little trace of primary texture or structure. It typically contains abundant quartz veins, many of which have been stretched and rotated, or transposed by isoclinal folding, into the plane of the principal schistosity. The latter is defined by oriented chlorite and mica, and by small-scale differentiation of quartz and sheet silicates. Garnet and glaucophane are commonly visible in the field. Mineral proportions are variable but a representative composition is about 30% white mica, 30% albite, 25% quartz, 15% mafic minerals (chlorite, glaucophane and garnet), and accessory epidote, opaque ore, rutile, sphene, tourmaline and zircon. Jadeitic pyroxene and chloritoid occur rarely.

(iii) *Mafic rocks.* A sequence of rocks of dominantly mafic composition is interlayered with the grey schist at the top of the unit, around the lac de l'Arpont, and this sequence is duplicated by a thrust in that area (Figs. 4–6). Blue glaucophane schist and green chlorite–albite schist are interlayered on a scale of several tens of metres: either type may be massive or schistose. Porphyroblasts up to 2 mm of garnet and albite are widespread, and epidote, white mica, green biotite, sphene and ore minerals may also be present. Some layers contain blocky mafic megacrysts up to 2 mm across: these may be single crystals of glaucophane, or in the green rocks, aggregates of actinolite replacing hornblende. The blocky habit of these megacrysts

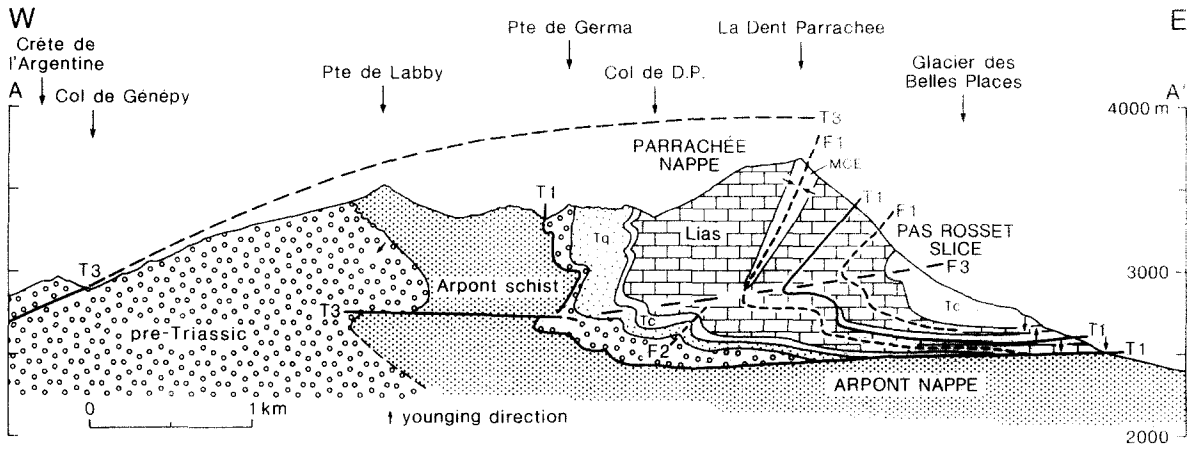

Fig. 3. Sketch section A–A' across the southern Vanoise massif, to show the tectonic situation of the Arpont nappe. For location see Fig. 2. T1, main nappe contacts; T3, backthrusts; F1, etc. major folds; Tq, Triassic quartzite; Tc, Triassic carbonate rocks. MCE; Upper Jurassic (Malm). Cretaceous, and Eocene. Arrows, younging directions determined from sedimentary structures or from stratigraphic sequences containing three or more dated units.

suggests that they may originally have been igneous phenocrysts (possible pyroxene), which have been successively replaced during pre-Alpine and Alpine metamorphism. There are also interlayers up to 5 m thick of a distinctive yellow-weathering silicic rock, which form useful marker horizons (Figs. 5 and 6). The rock is composed of fine-grained quartz, albite, epidote and white mica, and may contain garnet, glaucophane, chlorite, green biotite, stilpnomelane and ore.

The megacrysts and the pronounced layering in some of the mafic rocks suggest that they may originally have formed a layered intrusive complex. The silicic layers may have been aplite dykes. Rocks with these characteristics are shown as "gabbro" and "aplite" on the maps and cross-sections. Where the primary texture has been obliterated, the mafic rocks are shown as "glaucophanite" or "chlorite-albite schist", according to the dominant mineral assemblage.

(iii) *Metagranitoid.* A small body of deformed granitic rock (Figs. 4–6) consists of fully recrystallized quartz, sodic plagioclase, microcline, white mica, and accessory carbonate, green biotite and zircon. Saliot (in Goffé 1975) has reported jadeite from this body.

Pre-Triassic sedimentary sequence

The bulk of this sequence consists of massive coarse-grained metasandstone and metaconglomerate with visible detrital quartz and feldspar. Some of the pebbles are of pink quartz, which Ellenberger (1966) considers characteristic of the Permo-Triassic. There are interlayers of green chlorite–actinolite–albite schist, presumably of mafic volcanic origin, grey chlorite schist, and white or pale green quartz–phengite phyllite. The latter varies in composition from almost pure quartzite to almost pure phengite schist, and appears to show a stratigraphic transition into the widely recognized lower Triassic quartzite, which suggest that it is the youngest part of the Permo-Triassic succession. Tourmaline and ankerite are conspicuous accessories in all these rocks. The lack of garnet is useful in distinguishing them from the Arpont schist.

An inverted pre-Triassic sequence is exposed on the west side of the Vanoise massif (Figs. 2 and 3). It consists mainly of chlorite–albite schist, but includes beds of pebble conglomerate showing channelling and grading, indicating the younging direction. At the stratigraphic base of the sequence there are several tens of metres of boulder conglomerate, with clasts of vein quartz and of schist that was foliated before deposition of the conglomerate. This sequence apparently lies non-conformably on the Arpont schist, suggesting that it is part of the Arpont nappe. Chlorite pseudomorphs after what may have been a sodic amphibole are present in these rocks (Goffé 1975).

Triassic–Eocene sedimentary sequence

Apart from pure white quartzite of assumed lower Triassic age, the Triassic–Eocene succession consists of carbonate rocks and calcareous slates. Ages have been determined on palaeontological grounds by Ellenberger (1958). Dominant metamorphic mineral assemblages are of the greenschist facies, and include calcite, dolomite, quartz, white mica, chlorite and albite. Relict HP/LT minerals include crossitic blue amphibole (Bocquet 1971), lawsonite pseudomorphs (Ellenberger 1960), and Fe,Mg-carpholite + chloritoid (Goffé 1977, 1982).

STRUCTURE

The Arpont nappe, like much of the Pennine region, has undergone a complicated polyphase deformation history. Our purpose in studying this history in detail and in describing it here is to help relate the metamorphic and microstructural data to the tectonic evolution. Metamorphic mineral assemblages and microstructural data on deformational processes can be related in thin section to foliations and lineations. Mesoscopic structural analysis can then be used to relate these fabrics to large-scale structures.

The structural history described below was set up on

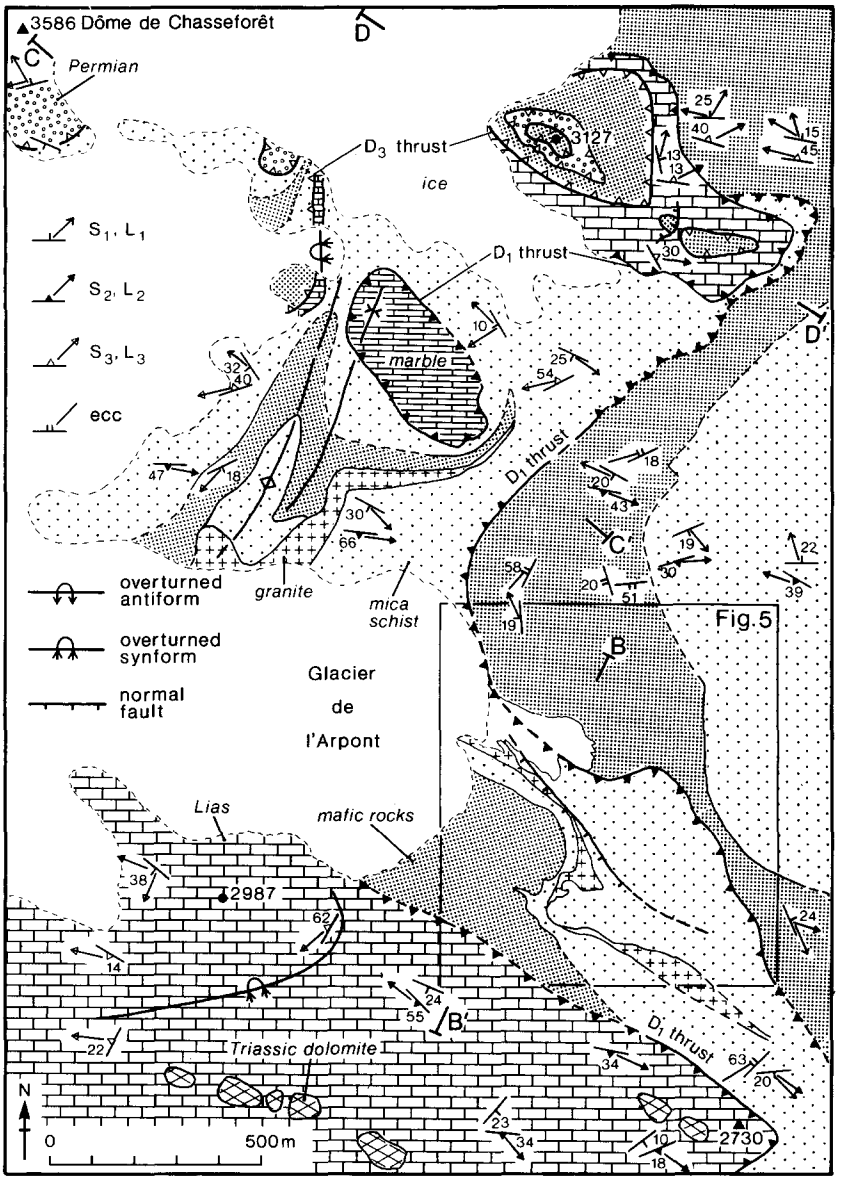

Fig. 4. Structural map of the Arpont area. See Fig. 2 for location. ecc, extensional crenulation cleavage and associated intersection lineation; open stipple, quartz–mica schist; close stipple, mafic rocks; crosses, metagranite; circles, presumed Permian quartz–phengite schist; cross-hatch, Triassic dolomite; large bricks, Liassic limestone; small bricks, marble with dolomite bands, probably Triassic.

the basis of detailed work in a small area of excellent exposure around the Glacier de l'Arpont. The temporal relationships among various small-scale structures were established on individual outcrops using overprinting relationships. We then correlated sets of structures within the study area using several criteria, including the classical ones of orientation, style, and position in locally established temporal sequences. The most important field technique, however, involved continuous tracing of fabrics or sets of structures across areas of good exposure. This allowed us to detect major changes of orientation and style caused by strain variation within a single deformation, for example, or by modification during later events. We also found that a single set of structures in one locality might be represented by two or more sets of progressively developed structures in another, and that certain sets of structures are only locally developed.

Using standard petrographic techniques, we established the microstructural characteristics of the various fabrics and their relationship to metamorphic mineral growth, and made interpretations about the deformational mechanisms that operated during each event. This then allowed us to make spot checks on our field correlations, particularly where the tracing technique was impossible because of poor exposure.

Using these methods we distinguished three major groups of structures, which we believe may represent distinct episodes of deformation (D_1, D_2 and D_3), at least in this area. Structural data are presented on the maps (Figs. 4 and 5), sections (Figs. 6–8) and equal-area plots (Fig. 9).

D_1

Much of the grey schist in the nappe has a strong regionally flat-lying foliation (S_1) defined by oriented

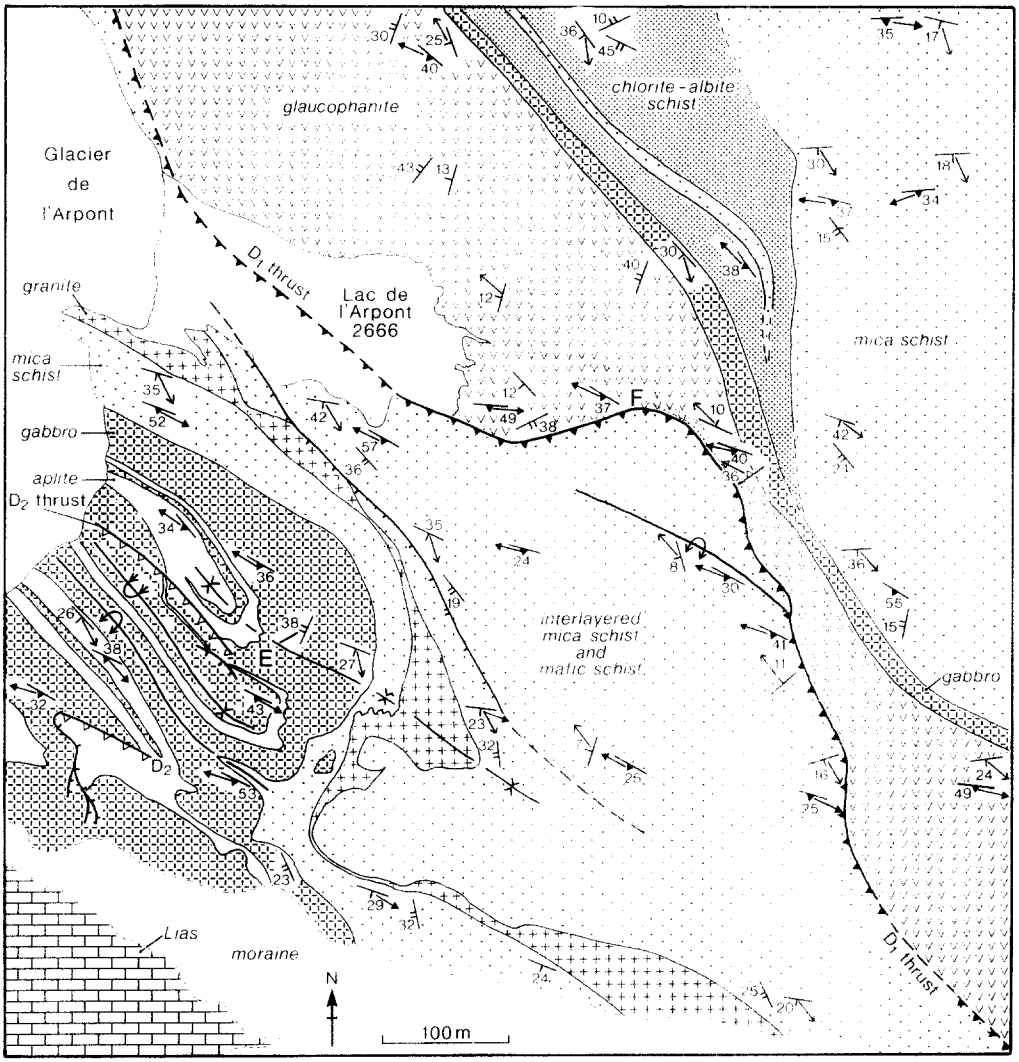

Fig. 5. Structural map of the area at the foot of the Glacier de l'Arpont. See Fig. 4 for location and structural symbols. E, location of Fig. 10(a); F, location of Figs. 10(b), (c), (d) and 11(b).

mica and chlorite and differentiated layering of quartz and sheet silicates on a 0.5–2 mm scale. The abundant quartz veins have been isoclinally folded, or stretched and rotated, so that they lie roughly parallel to this foliation. Glaucophane is strongly lineated in the foliation, and this lineation has a remarkably consistent orientation, trending 320° with a spread of less than 50° in azimuth (Fig. 9a). This may have been the maximum finite elongation direction caused by D_1. S_1 is also the dominant foliation in glaucophane schist. D_1 folds of layering are rare (Fig. 10a), and hence orientation data are lacking.

D_1 structures are the earliest that we have recognized in the field, and S_1 is commonly the dominant foliation. D_1, however, is certainly not the earliest deformation to have affected these rocks. Microstructural evidence described below indicates that at least one and possibly several deformational events, including pre-Alpine events, preceded D_1.

We have not been able to relate the mesoscopic D_1 structures unequivocally to larger-scale features. Several major structures clearly predate D_2, however, and may therefore have formed during D_1. The mafic rocks around the lac de l'Arpont have been duplicated by thrusting along a shear zone up to 5 m thick (Figs. 4–6), which is occupied by discontinuous slices of green quartz–phengite phyllite and grey chlorite–phyllite (probably Permian) and white quartzite (Trias) with a strong S_1 foliation. This thrust is folded by D_2 folds (Figs. 6 and 10b). No small-scale indicators of the sense of displacement are preserved. The thrust cuts up to the upper surface of the schist towards the north, however, suggesting displacement in roughly that sense. The NW-trending glaucophane lineation in the schist may also approximate the movement direction. The thrust places schist over Permian metasediment in the shear zone over a N–S distance of 5 km, which provides an indication of the minimum displacement.

Near the southern termination of the schist, south of La Dent Parrachée (Fig. 2), there are several interleaved slices of Arpont schist and Permian. The area has been affected by intense D_2 and D_3 deformation, but some of these slices may be of D_1 age.

The inversion of the Mesozoic rocks above the Arpont Schist also occurred before D_2, as D_2 folds have the same orientation and sense of asymmetry above and below the

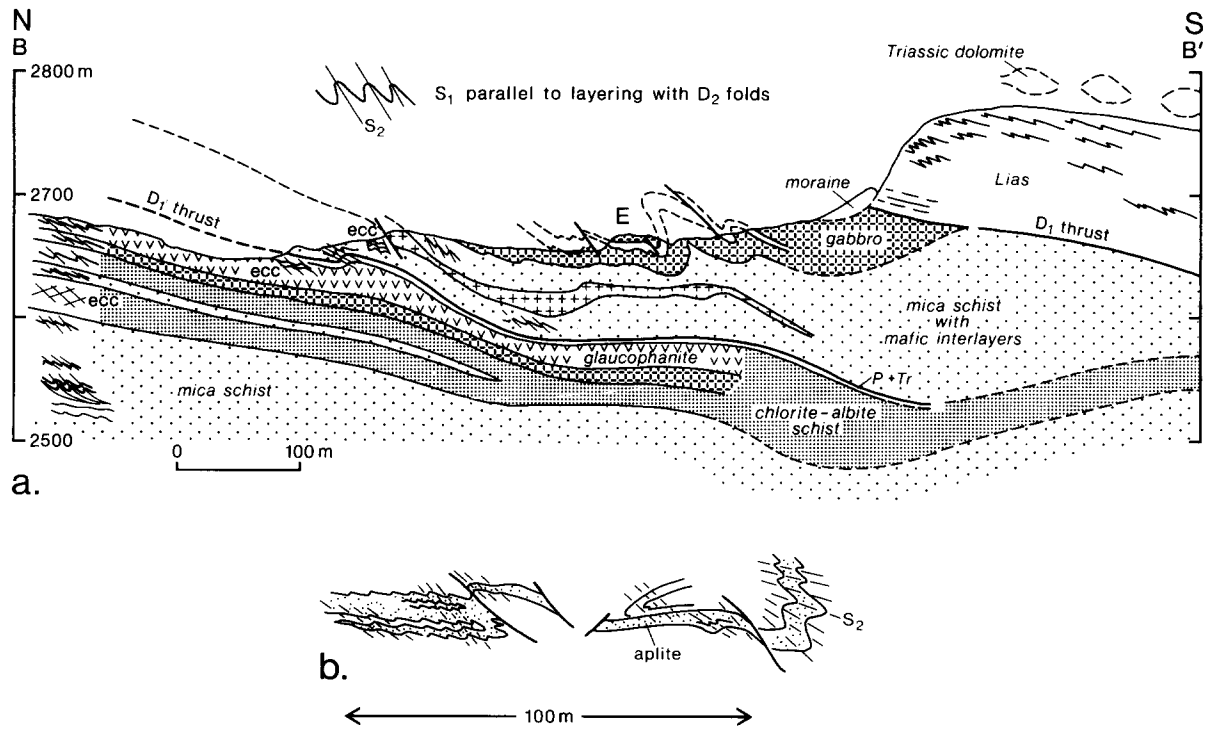

Fig. 6(a) Structural section B–B′ to illustrate D_1 and D_2 structures. See Fig. 4 for location. ecc, extensional crenulation cleavage; P + Tr, presumed Permian and Triassic metasediments along the D_1 thrust. E, location of inset. (b) Detail of D_1 and D_2 folds in aplite and metagabbro layers at location E.

contact (Fig. 6). This inversion is associated with the major nappe structures in the Mesozoic shown in Fig. 3, which are also of D_1 age (Platt & Lister, in review). The contact is marked by a thin band of calc-mylonite, the microstructure of which is partly obscured by secondary recrystallization and grain growth. The elongation lineation in the mylonite trends between 105 and 120°, but its precise age and the sense of displacement are unclear.

D_2

Layering and S_1 in the upper part of the nappe have been thrown into a distinctive set of tight cylindrical N-vergent folds with E–W axes and S-dipping axial planes (Figs. 6 and 9b). These are associated with a variably developed crenulation cleavage, S_2, which transposes S_1 and becomes the dominant foliation in zones of strong D_2 deformation. Transposition can occur over a distance of a few cm (Fig. 10d): nowhere can the age of the dominant foliation be assumed without careful examination. There is a strong lineation L_2 parallel to fold axes: this is partly a crenulation lineation, and is partly caused by the intersection of S_2 differentiation bands with S_1. No clearcut indication of the maximum elongation direction during D_2 is developed. D_2 in mafic rocks commonly obliterates the mesoscopic S_1, and this can give the rock a structureless appearance: massive blue and green mafic rocks, apparently undeformed, show strongly crenulated S_1 in thin section. Where D_2 is strong in mafic rocks, however, it has produced strongly foliated chlorite–albite schist. D_2 effects appear to be mainly restricted to the uppermost part of the nappe: 500 m below the upper contact, effects are scarcely detectable, whereas in the mafic rocks forming the top 100 m around the lac de l'Arpont, S_2 is the dominant foliation in broad zones. We have found no major structures provably related to D_2 in the Arpont area.

D_3

Local S- to SE-vergent folds and crenulations are developed around the lac de l'Arpont, with W to SW-trending axes and W to N-dipping axial-planes (Fig. 9c). These overprint D_2, and microstructural evidence suggests that D_2 and D_3 structures are distinct events separated by a hiatus. North (Dôme de Chasseforêt) and south (La Dent Parrachée) of Arpont the intensity of D_3 increases upward into the axial zone of a major W-closing synform (Figs. 3 and 7), that folds the entire nappe. The axial planes of the crenulations fan into a horizontal position in the overturned limbs of these folds (Fig. 7). In this area we distinguish two sets of crenulations, both of which are spatially associated with the same major structure (Fig. 7b).

During D_3, slices of Arpont schist were thrust eastwards over the Mesozoic rocks of the overlying nappes (Fig. 8). These folds and eastward-directed thrusts appear to be related to the backfolding and backthrusting events widely recognized in the French and Swiss Alps (Debelmas 1976, Milnes *et al.* 1981).

Extensional deformation

Sets of distinctive non-penetrative structures formed by horizontal extension are widespread in the Arpont schist. These clearly overprint D_2 structures, but their

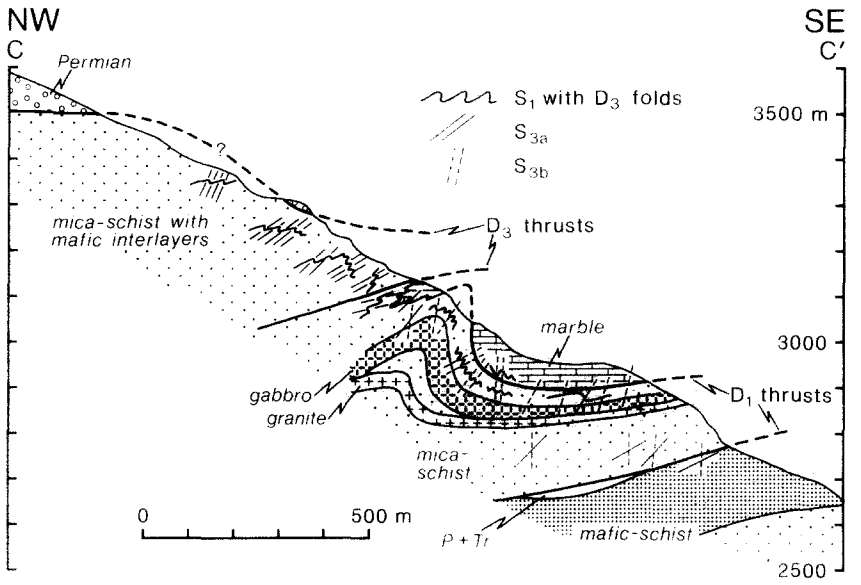

Fig. 7. Structural section C–C′ to illustrate D_3 structures. See Fig. 4 for location. Two crenulation cleavages, S_{3a} and S_{3b}, are developed around the larger-scale folds. S_{3b} is the younger.

relationship to D_3 is not clear. The structures include boudinage of competent layers, foliation boudinage, and extensional crenulation cleavage (Platt & Vissers 1980) in strongly foliated rocks. The latter is a crude spaced cleavage defined by sets of small-scale shear-bands that offset and extend the older foliation. The orientation of the cleavage is very variable, and at least two sets appear to be developed: one dips west or northwest, the other southeast (Figs. 5 and 9d). The sense of shear appears to be roughly downdip in each case. The NW-dipping set is widespread in the Arpont schist, and in mafic rocks is marked by narrow zones of alteration to ankerite and chlorite. Around the lac de l'Arpont, the SE-dipping set is largely restricted to the early thrust zone cutting the Arpont schist (Fig. 11a). This might suggest a genetic relation between the thrust and the cleavage (e.g. White *et al.* 1980) except that the thrust clearly predates D_2, and the cleavage overprints S_2 (Fig. 11b). The whole area, including the thrust, is warped by very open folds which strongly resemble the small-scale extensional crenulations (Fig. 11c and 14). The cleavages are most pronounced in SE-dipping limbs of these warps, suggesting that they are themselves large-scale extensional structures.

Possibly still later, unrelated, structures include W-dipping shear zones with down-dip displacements, which are associated with ankerite veins and alteration in the mafic schists of the Arpont area. These may be related to the major N-trending faults and downwarps that bound the Vanoise culmination on the west side.

METAMORPHISM AMD MICROSTRUCTURE

Our interpreted history of mineral growth and deformation is summarized in Table 1. The basis for these interpretations is discussed below.

D_1

In thin-section, S_1 is defined by oriented glaucophane, white mica, and chlorite, and in quartz-rich rocks by differentiation of quartz relative to amphibole and sheet silicates. Glaucophane also defines L_1, but its orientation is imperfect, and some grains lie in S_1 oblique to L_1, and others stand at high angles to the foliation. S_1 wraps around the latter (Fig. 11d), suggesting that they predate D_1. Where S_1 is weak, the glaucophane commonly forms radiating rosettes which have grown statically over an earlier (pre-Alpine?) foliation. Deformed relics of these rosettes are locally preserved between the S_1 foliae. Some crystals have also been broken and extended parallel to S_1 and L_1 (Fig. 12a). The microstructure suggests that much of the prismatic glaucophane predates D_1, and that D_1 strain has mechanically rotated it into statistical parallelism with the schistosity and linea-

Table 1. Inferred stable mineral assemblages in the Arpont schist during its deformational and metamorphic history

	Quartz–mica–schist	Mafic schist
D_3	qtz + w.m. + chlor	Chlor + ab + w.m. + carbonate minerals (disequilibrium)
thermal peak	qtz + w.m. + chlor + ab	Chlor + green bi + ab + epi? ± calcite? + sphene
D_2	qtz + w.m. + chlor + ab?	Chlor + ab? + epi + w.m. + sphene
D_1	qtz + w.m. + glauc	Glauc + epi + w.m. + sphene
Pre-D_1 (Alpine)	qtz + w.m. + glauc ± jadeitic pyroxene? ± chloritoid?	Glauc + lawsonite + sphene?
pre-Alpine	qtz + w.m. + garnet	Hornblende + garnet + rutile

□ Abbreviations: ab, ablite; bi, biotite; chlor, chlorite; epi, epidote; glauc, glaucophane; qtz, quartz; w.m., white mica. These assemblages are not necessarily complete. Question marks mean that the textural relationships have not been clearly established.

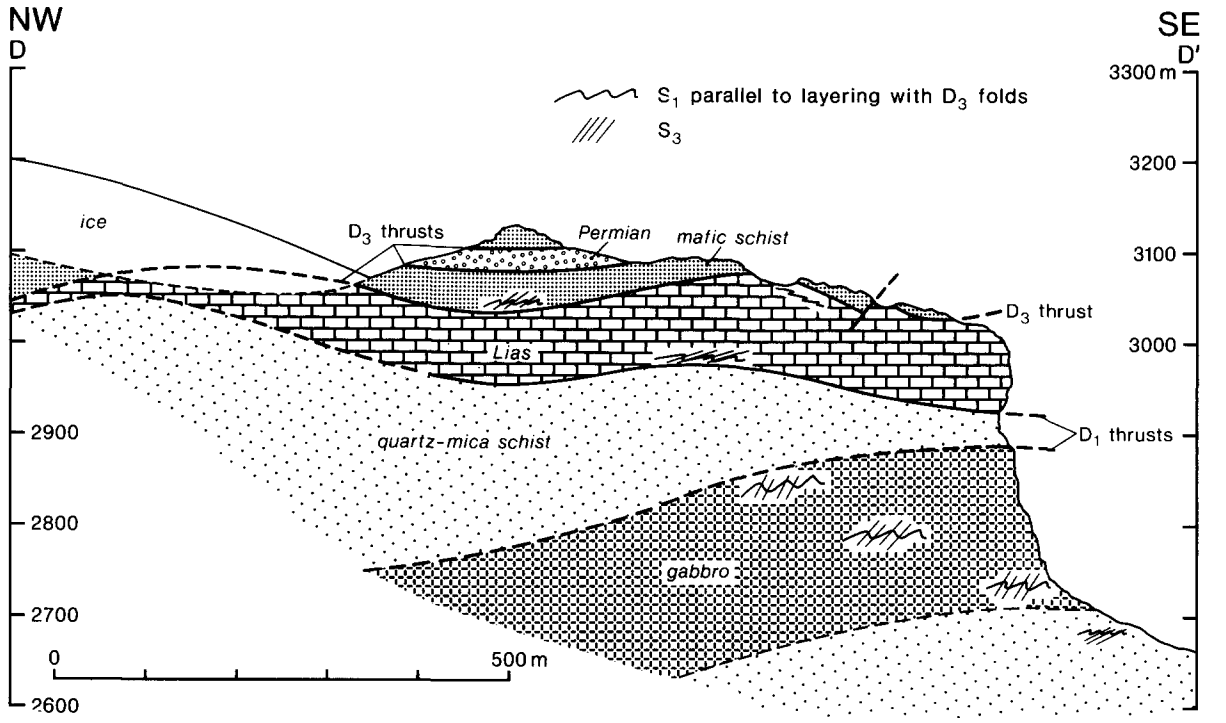

Fig. 8. Structural section D–D′ to show effects of D_1 and D_3 thrusting. See Fig. 4. for location.

tion. There is also evidence, however, for recrystallization and growth of glaucophane during D_1. Blocky glaucophane megacrysts in some mafic schists act as augen predating S_1, but the grains are marginally deformed and recrystallized to finer grained glaucophane lying in S_1. Glaucophane has also formed in cracks in garnet, growing parallel to L_1 (Fig. 12b).

White mica and well-formed oriented epidote prisms lie in S_1 and are likely to have been stable at that time. The mica orientation in some samples has been produced by crenulation and transposition of an earlier (pre-Alpine?) fabric, accompanied by recrystallization during D_1. Chlorite and green biotite are also commonly parallel to S_1, and help to define it, but these minerals clearly replace glaucophane (Fig. 13d), and in view of the evidence for stability of glaucophane during D_1, it is likely that this alteration is later. The interpreted stable mineral assemblages during D_1 therefore include quartz + white mica + glaucophane (in metasediments), and glaucophane + epidote + white mica + sphene (mafic schist).

Even in rocks that have undergone no post-D_1 deformation, these microstructures have been obscured by grain boundary migration and grain-growth in quartz to establish minimum surface-energy ('foam') textures, by alteration of garnet and glaucophane to chlorite and green biotite, and by growth of albite. Nevertheless, the preserved evidence suggests that D_1 deformation involved crenulation of an earlier mica fabric, grain rotation, and diffusional mass-transfer of silica (pressure-solution) to produce a differentiated foliation. This was accompanied by recrystallization and growth of white mica and glaucophane.

Pre D_1 events

Pre-D_1 minerals include garnet and glaucophane. Bocquet (1974b) has documented a pre-Permian amphibolite-facies metamorphic event in the Arpont schist, and the garnet is most likely to have formed synkinematically during this event (Fig. 12c). We have found no evidence for Alpine garnet in the area (cf. Goffé 1975), and garnet is lacking in the Permian and younger rocks.

The pre-D_1 glaucophane described above presumably grew during a relatively early Alpine high-pressure metamorphism in the Arpont schist. Some mafic schists also contain rectangular or six-sided pseudomorphs, consisting of fine-grained epidote-group minerals, carbonate, white mica, and chlorite (Fig. 12d). The habit and replacement products suggest lawsonite as the precursor. As epidote was apparently stable during D_1, the lawsonite probably predates it. Jadeitic pyroxene has been found in quartz–mica schist by Bocquet (1974) from the Arpont area, and she kindly allowed us to examine her samples. Coarse prismatic jadeite occurs with quartz in a vein that has subsequently been folded, and it also occurs with quartz, white mica and glaucophane in metasedimentary schist, where it is oriented in statistical parallelism with a foliation resembling S_1. We saw no evidence that the jadeite crystallized at the expense of a high-temperature igneous felspar, as suggested by Saliot (1979). We therefore tentatively conclude that pre-D_1 high-pressure assemblages included quartz + white mica + glaucophane ± jadeitic pyroxene in metasediments, and glaucophane + lawsonite + sphene in mafic schist.

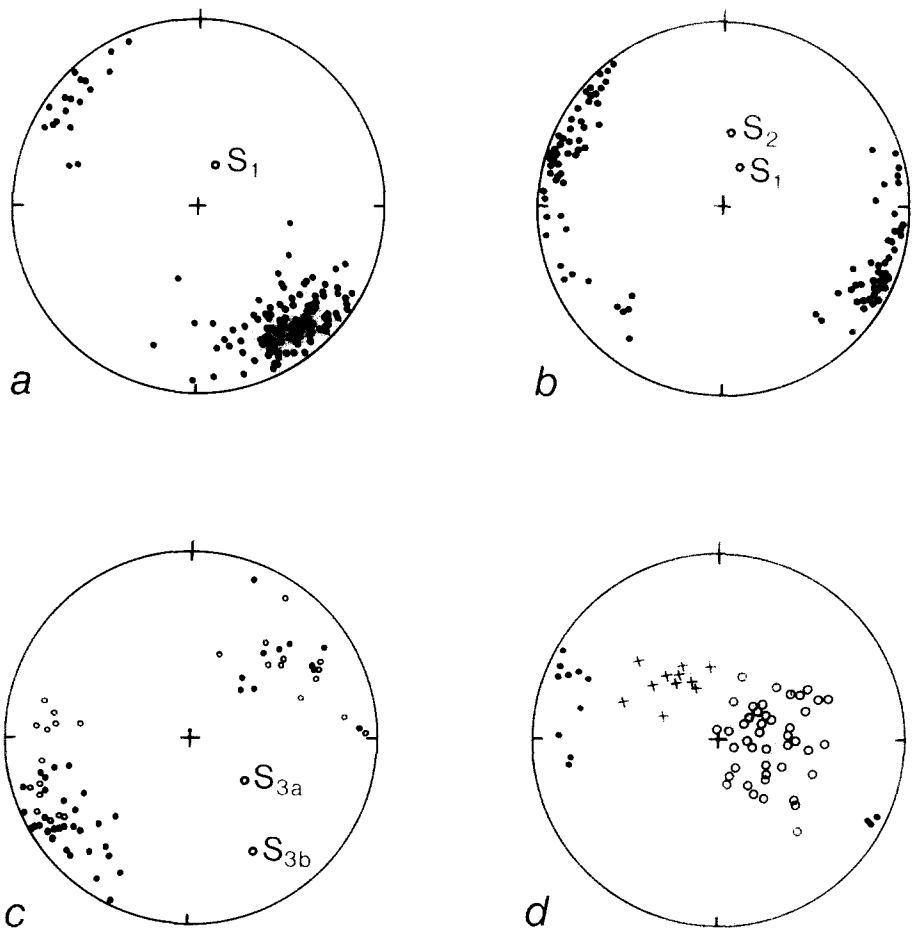

Fig. 9. Orientation data, Arpont area. (a) Glaucophane lineation L_1. Mean of S_1 (150 readings) is shown. (b) Crenulations and minor fold axes L_2. Means of S_1 and S_2 (110 readings) are shown. (c) Crenulations and minor fold axes L_3, from the western slopes of the Dôme de Chasseforêt (Fig. 4). Two sets are distinguished: D_{3a} crenulations (closed cirlces) are locally overprinted by D_{3b} (open circles). Means of S_{3a} (26 readings) and S_{3b} (28 readings) are shown. (d) Extensional crenulation cleavages. Open circles, W or NW sense of slip; crosses, SE sense; closed circles, intersection lineations related to NW-slip set.

D_2

D_2 caused crenulation and substantial modification of S_1 in many rocks. Glaucophane was mechanically rotated, and in extreme cases transposed into S_2 (Fig. 13a). The crystals are sometimes bent and broken in the crenulation hinges, but they may also occur as unstrained prisms bound by straight (110) prism faces. These could be interpreted as indicating recrystallization of glaucophane during D_2. In view of the evidence for instability of glaucophane during D_2, however, we suggest that these grains are simply cleavage fragments that subsequently drifted apart from each other during dilation and differentiation of quartz into the crenulation hinges. Alteration of glaucophane to chlorite is extensive, particularly along S_2 cleavage zones, and the rocks most strongly affected by D_2 have mostly been completely reconstituted to chlorite–albite schist. White mica was crenulated, and has recrystallized in crenulation hinges (Fig. 13b). Albite is mainly post D_2, as it grows helicitically over D_2 crenulations (Fig. 13c); but the breakdown of glaucophane during D_2 is also likely to have caused albite growth at that time. The interpreted mineral assemblages during D_2 therefore include quartz + white mica + chlorite + albite (metasediments), and chlorite + albite + epidote + white mica + sphene (mafic schist).

Extensive differentiation of quartz relative to sheet silicates and glaucophane occurred during D_2 (Fig. 13a), and chlorite has filled in pull-apart voids in crenulated mica schist. Deformation was therefore achieved by crenulation and diffusive mass-transfer of quartz and chlorite. The mobility of chlorite was probably a result of the instability of glaucophane, which was breaking down to release Mg, Fe and Al. This metamorphic reaction may therefore have contributed to the ductility of the rock during D_2.

Inter D_2–D_3 thermal peak

Extensive growth of albite porphyroblasts occurred after D_2, and before D_3, in both the Arpont schists and the overlying Mesozoic rocks. Their relation to older and to younger fabrics provides a useful time-marker for correlating deformational events. The porphyroblasts grew helicitically over all earlier fabrics (Fig. 13c), and involved extensive diffusion, not only of albite components, but also of the material the albite replaces (mainly

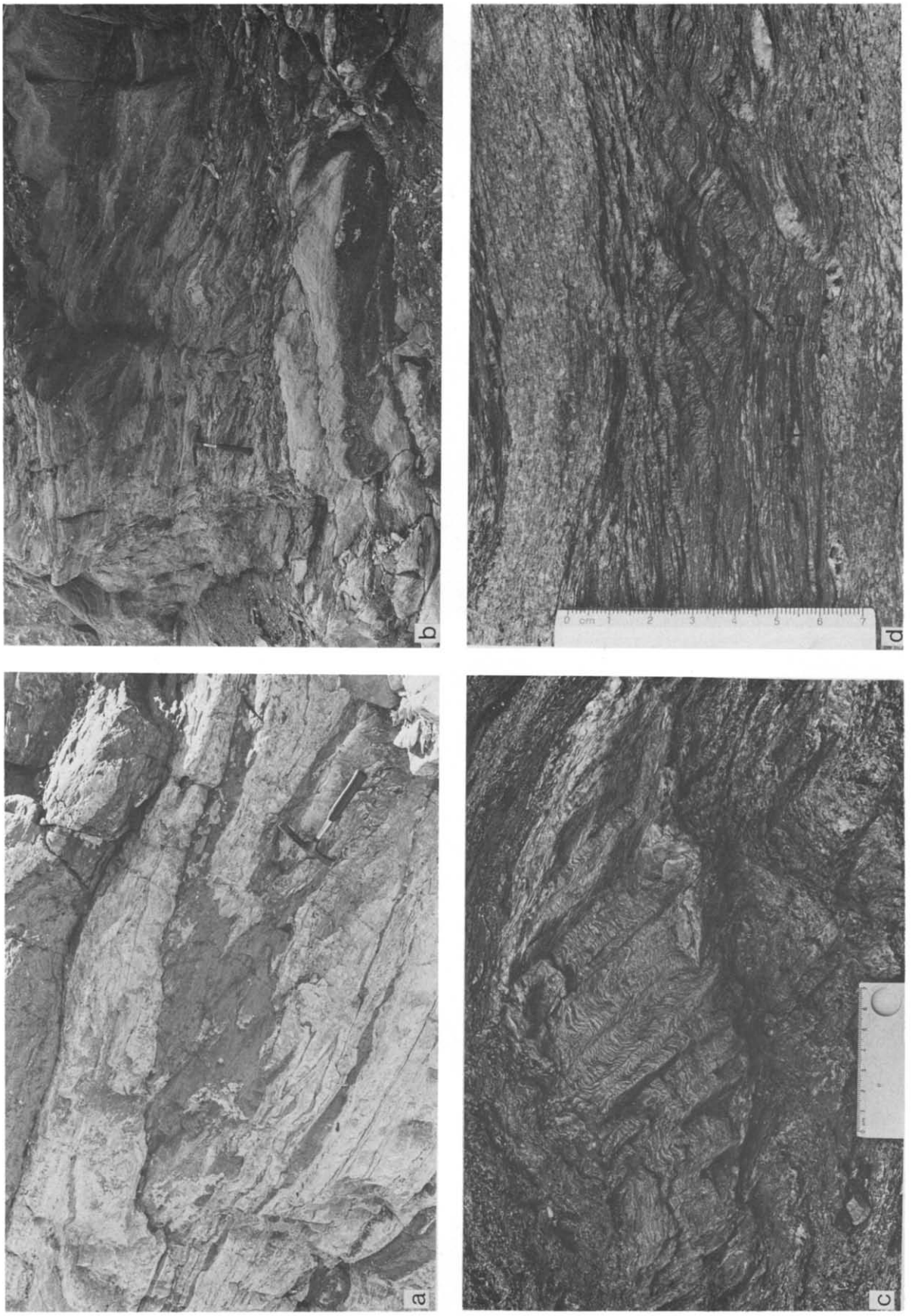

Fig. 10(a) F_1 fold refolded by F_2 in meta-aplite and meta-gabbro, location E in Figs. 5 and 6. Looking E. (b) D_1 thrust zone, location F in Fig. 5. Massive rock at very top is Arpont schist, the rest is Permian phyllite in the thrust zone. Note strong small-scale D_2 folds which post-date the thrust. Looking E. (c) D_2 crenulations: detail from Fig. 10(b). Note strongly differentiated foliation S_1, and incipient spaced cleavage S_2. (d) Marked variation in orientation and style of S_2 crenulation cleavage, in D_1 thrust-zone, location F. Open ripples at right with axial planes dipping 45°S pass into tight crenulations with axial planes dipping 10°S at left. The cleavage S_2 at left is almost indistinguishable from S_1. Looking W.

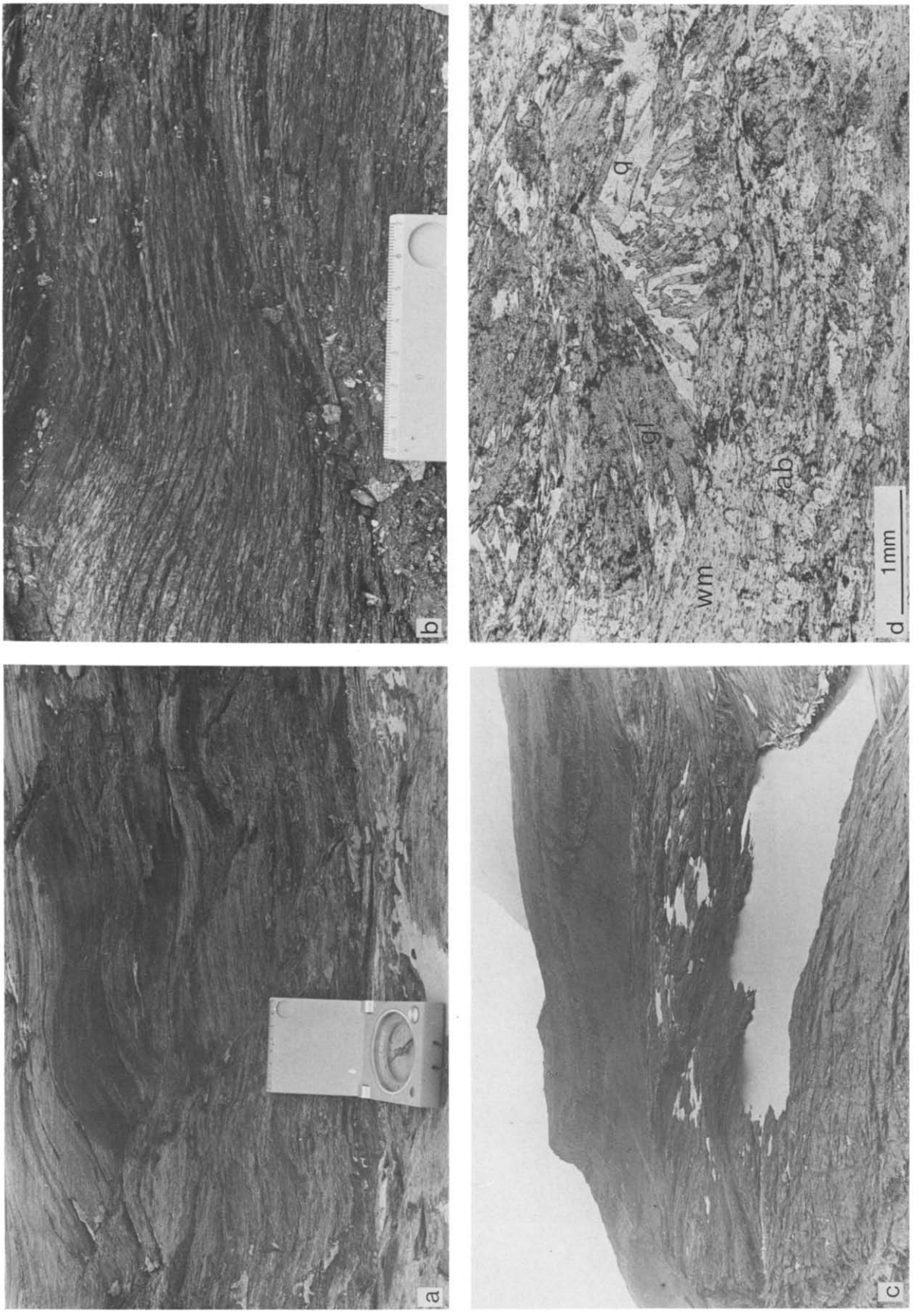

Fig. 11(a) NW-dipping extensional crenulation cleavage in mafic schist. The horizontal foliation is S_1. Looking SW. (b) SE-dipping extensional crenulation cleavage zone in Permian quartz-plagioclase phyllite, location F. The cleavage zone deforms and offsets S_2 crenulation cleavage, which is the main foliation. Looking W. (c) Lac de l'Arpont area, showing large-scale extensional warps in Arpont schist. Ridge of Liassic limestone in the background. See Fig. 14 for interpretative sketch. Looking S. (d) Photomicrograph: S_1 foliation defined by glaucophane, showing deformed relic of pre-D_1 glaucophane rosette. Section parallel to L_1. ab, albite; gl, glaucophane; qtz, quartz; wm, white mica.

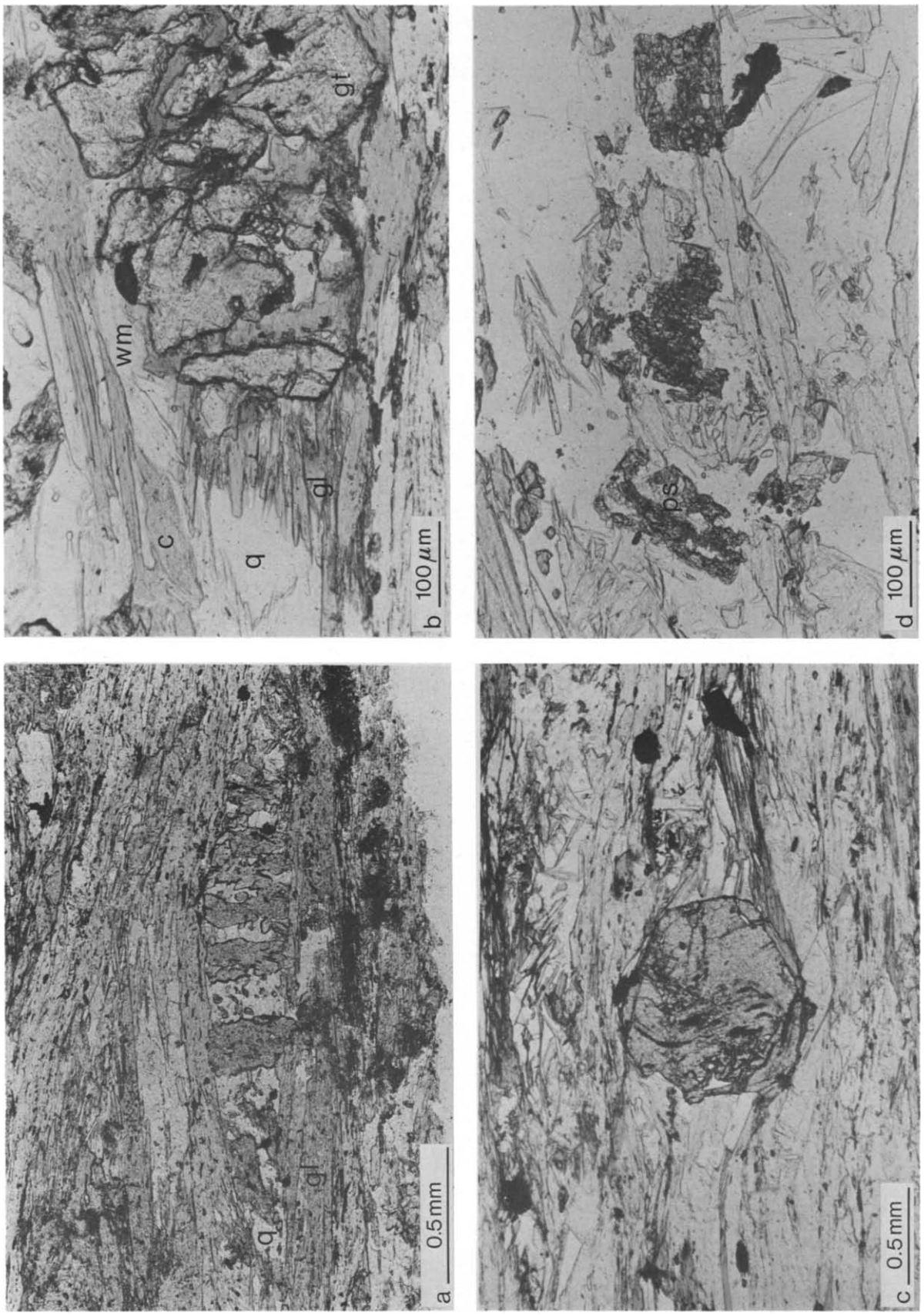

Fig. 12. Photomicrographs. (a) Glaucophane crystal pulled apart parallel to S_1 and L_1. Section parallel to L_1. (b) Pre-Alpine garnet broken and partly replaced by glaucophane during D_1. Glaucophane at left has grown parallel to S_1 and L_1. Section parallel to L_1. c, chlorite; gt, garnet; gl, glaucophane; q, quartz; wm, white mica. (c) Pre-Alpine garnet in grey quartz–mica schist with rotational inclusion trails. The external foliation is S_1, which truncates the internal fabric in the garnet. (d) Possible pseudomorphs after lawsonite (ps): see text for discussion.

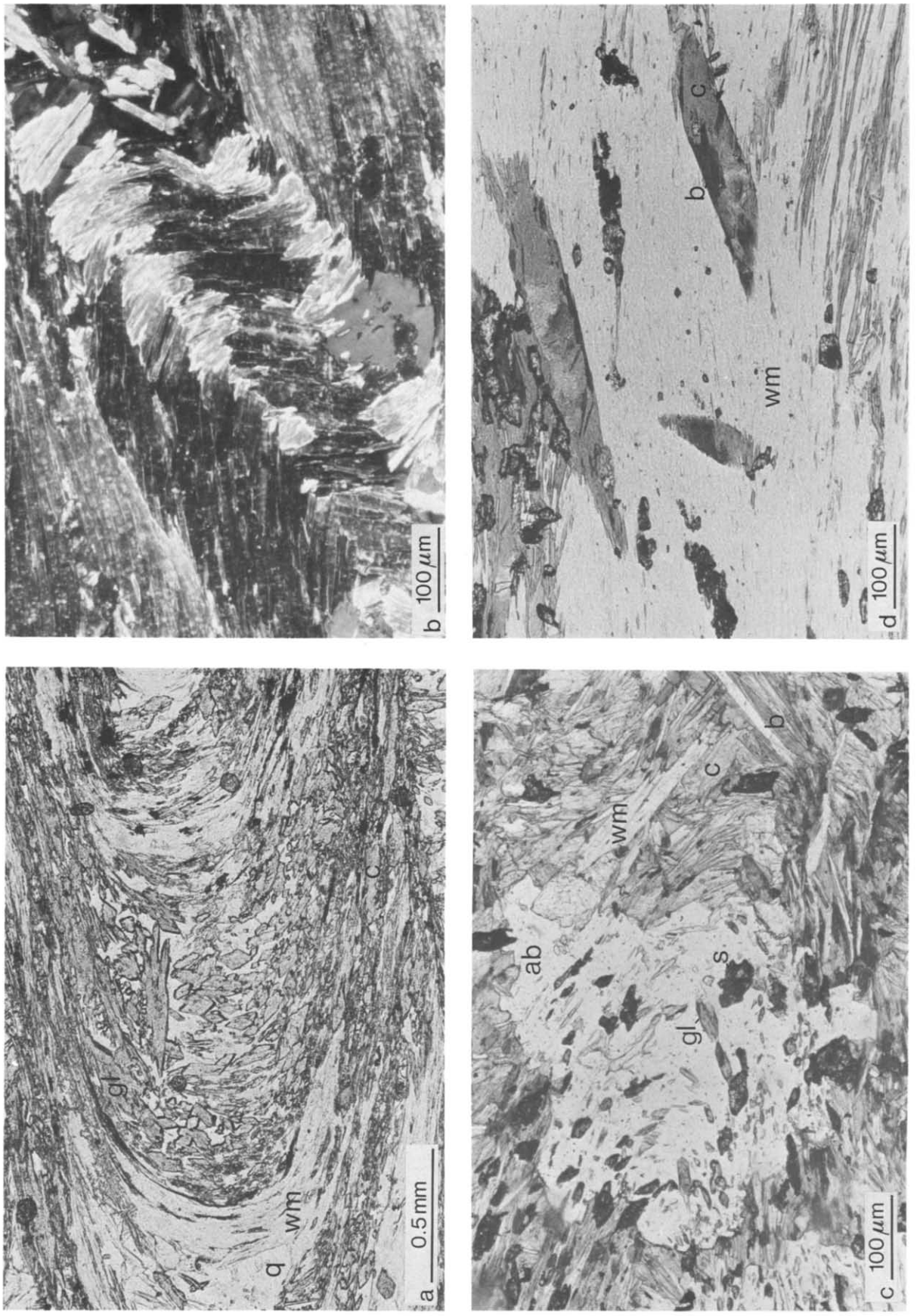

Fig. 13. Photomicrographs. (a) D_2 crenulations of the S_1 foliation defined by glaucophane. Note cleavage fragments 'floating' in the quartz that has been differentiated into the microlithons. There has been considerable replacement of glaucophane by chlorite (c) in the S_2 cleavage zones. Section normal to L_2. (b) D_2 crenulations in mica–schist. Note recrystallization in the crenulation hinges. Section normal to L_2. (c) Albite porphyroblast that has grown helicitically over a D_2 crenulation, defined by relict glaucophane (gl), white mica (wm) and sphene (s). Glaucophane outside the albite has been completely replaced by chlorite (c) and biotite (b) in this sample. Section normal to L_2. (d) Pseudomorphs of glaucophane replaced by chlorite and green biotite, which have grown in crystallographic continuity with the white mica outside the pseudomorphs.

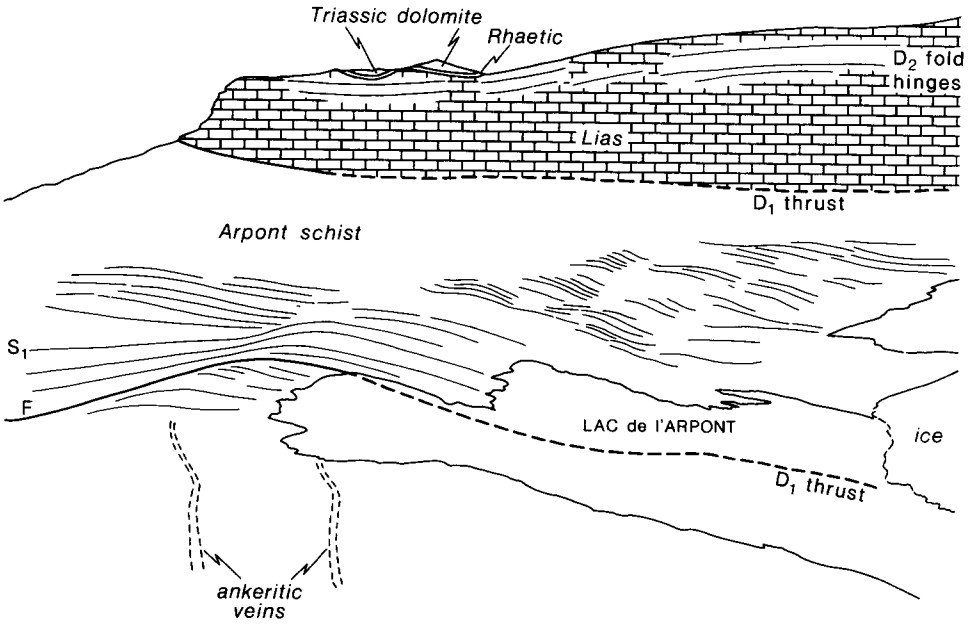

Fig. 14. Sketch of the lac de l'Arpont area, to show large-scale open warping of the foliation (drawn from Fig. 11c). Compare this structure with the extensional crenulation cleavage illustrated in Figs. 11(a) and (b). F: location of Figs. 10(b)–(d) and 11(a)–(b). Note late shear-zones with ankerite veins.

chlorite and white-mica). By replacing minerals that defined earlier fabrics, albite growth has rendered many rock-types relatively massive. Much of the glaucophane was probably replaced by chlorite and green biotite during this post-D_2 event, as undeformed pseudomorphs (Fig. 13d) occur in rocks with considerable D_2 deformation. Also, albite porphyroblasts include unaltered glaucophane crystals defining D_2 crenulations (Fig. 13a) in rocks where no glaucophane remains outside the albite. Interpreted stable mineral assemblages in this event include quartz + white mica + chlorite + albite (metasediments), and chlorite + green biotite + albite + epidote ± calcite + sphene (mafic schist).

D_3

Ductile deformation in the Arpont schist during D_3 and later events was limited and not accompanied by extensive recrystallization and grain growth. S_3 cleavage zones in mafic schist are occupied by a disequilibrium assemblage of chlorite, white mica, albite and carbonate minerals. In the axial zones of the major D_3 folds, the older foliations are strongly kinked and crenulated, and irregular or stylolitic pressure solution seams marked by concentrations of opaques form a crude cleavage. These seams wrap around and hence postdate the albite porphyroblasts. The Permian–Eocene rocks of the area, on the other hand, were locally strongly affected by D_3, and lower greenschist-facies assemblages including chlorite and white mica were developed. S_3 in these rocks invariably postdates the large albite porphyroblasts formed in the post D_2 static event. D_3 therefore postdates the greenschist-facies thermal peak, and occurred well outside the stability field of the earlier HP/LT assemblages (cf. Caby *et al.* 1978, Goffé 1982).

TECTONIC SIGNIFICANCE OF THE METAMORPHIC HISTORY

The metamorphic history of the Arpont schist bears on its tectonic history in three very important respects, namely: (a) the tectonic relations between the Arpont schist and the surrounding Permian–Eocene metasediments; (b) the relationships between the high-pressure metamorphic event and formation of the nappe structures, and (c) the uplift history, as indicated by the trend to lower-pressure assemblages. A summary of our ideas on these problems is presented in Table 2, and we discuss the evidence below.

'Basement' and 'cover' relationships

As mentioned earlier, there has been some debate on the relation between the metamorphism in the Arpont schist and that in the surrounding rocks. Our contribution to this debate is not conclusive, but some of our

Table 2. Relations among deformation, metamorphism and tectonics in the Arpont Schist.

Deformation	Metamorphism	Tectonic significance
post D_3 warps and shear zones	low-grade alteration	differential uplift
D_3 and extensional phase	lowest greenschist facies	backfolding and backthrusting
	thermal peak: middle greenschist facies	thermal re-equilibration
D_2	lower greenschist facies	final emplacement of nappes?
D_1	glaucophane–epidote schist facies	ductile deformation, major nappe displacements?
pre D_1	high-pressure peak	underthrusting: subduction or collision. initiation of nappes?

observations are relevant. Firstly, the Arpont nappe is everywhere separated from the overlying Permian to Eocene sequence by a tectonic contact (Fig. 3). Secondly, the critical HP/LT assemblages jadeitic pyroxene + quartz and glaucophane + lawsonite predate the earliest recognizable deformation, and hence predate final emplacement of the nappes. Thirdly, we see no justification for ignoring the petrogenetic significance of the jadeitic pyroxene + quartz assemblage (cf. Saliot 1979, Goffé 1982). These points are compatible with Desmons' (1977) suggestion that the HP/LT metamorphism in the Arpont schist reached higher pressures and possibly predated that in the surrounding rocks.

Nappe emplacements and high-pressure metamorphism

Our structural and microstructural data suggest that the high-pressure peak in the Arpont schist predates the earliest and most important phase of ductile deformation (D_1), and by inference major displacements on the nappe contacts (Table 2 and Fig. 15). This leads us to the somewhat surprising conclusion that the visible structures and fabrics were not directly related to the tectonic process (subduction or collision) that caused deep burial and high-pressure metamorphism, but that they reflect the subsequent uplift history (cf. Caby *et al.* 1978, Goffé 1982).

The uplift history

The petrological evidence suggests a progression from HP/LT conditions before D_1 to a significantly lower pressure after D_2 (Fig. 15). The peak pressure of the pre-D_1 metamorphism, suggested by the assemblage jadeitic pyroxene + quartz, may have exceeded 10 kb (Desmons 1977). The progressive breakdown during D_1 and D_2 of the high-pressure minerals jadeite, lawsonite and glaucophane to form the post- D_2 middle greenschist-facies assemblage chlorite + green biotite + albite + epidote requires a drop of several kb pressure and possibly a slight rise in temperature (Fig. 15). A temperature rise by itself could not explain this sequence, as at 10 kb pressure there should be a direct transition from the blueschist facies to the albite–epidote amphibolite facies. The pressure drop suggests that D_1 and D_2 took place during uplift towards the Earth's surface, requiring the removal of 15 km or more of overburden. This may have been caused by erosion, by regional extension, or by some sort of tectonic denudation (e.g. gravity spreading). Whatever its cause, the structural evidence suggests that it coincided with substantial ductile deformation, and with major nappe displacements.

The progressive warming which led to the thermal peak between D_2 and D_3 was probably the result of thermal relaxation from an abnormally low gradient associated with underthrusting (England 1978). It may be related to the Lepontine thermal event in the Swiss Alps, and if synchronous, provides an absolute time marker at about 38 ± 2 Ma: Late Eocene–Early Oligocene (Desmons 1977).

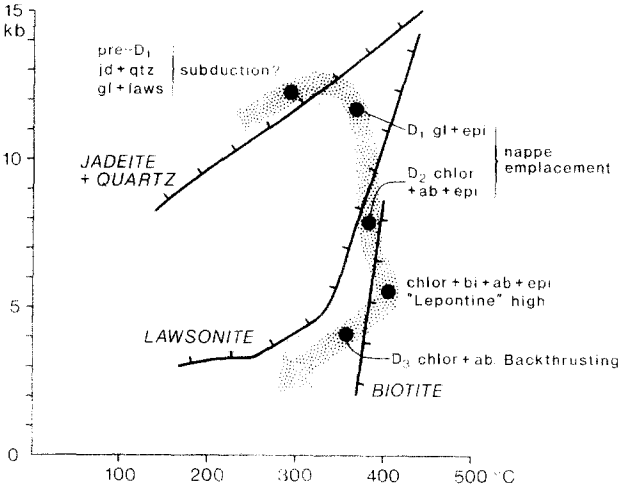

Fig. 15. P/T history of the Arpont schist. The path shown is qualitatively correct but is only loosely constrained. Jadeite + quartz stability field from Newton & Smith (1967), lawsonite field from Newton & Kennedy (1963) and Liou (1971). Biotite field from Winkler (1974). ab, albite; bi, biotite; chlor, chlorite; epi, epidote; gl, glaucophane; laws, lawsonite.

KINEMATIC INTERPRETATIONS

D_1 produced a flat-lying foliation and a consistent NW-trending glaucophane lineation (Fig. 9a). The latter is likely to represent the finite elongation direction, and the foliation suggests nearly vertical shortening. Strain is not measurable, but the intensity of the fabrics suggests that it is large. The association of D_1 with the nappes suggests that there may have been a significant component of subhorizontal shear, in which case the lineation may approximate to the transport direction. In view of the regional evidence for the emplacement of metamorphosed rocks from the oceanic Piémont domain northwards and westwards onto the European continental margin, we suggest that D_1 involved a significant component of shear towards the northwest. D_2 folds trend WNW, and are consistently asymmetric and N-vergent. In the Arpont schist they are fairly non-cylindrical: fold axes have a spread of about 70° in azimuth (Fig. 9b). In contrast, individual D_2 folds in the overlying Liassic rocks are highly cylindrical, with a mean trend of 305°; and the overall spread of axes within the area of Fig. 4 is about 40° (Platt & Lister in review). This suggests that the bulk elongation direction during D_2 probably lay in the northwest quadrant. The S_2 foliation everywhere dips south (Fig. 9b), and the dip decreases with increasing D_2 strain, as indicated by the tightness of the folds and the intensity of S_2. This suggests a northward component of shear during D_2. We tentatively suggest, therefore, that D_2 in this area also involved a component of NW-directed shear, as this would explain the geometry of both the folds and the foliation. This inference is consistent with our suggestion that D_1 and D_2 may represent different stages in the formation and emplacement of the nappes.

Most of the structural evidence for the nature of D_3 comes from the nappes of cover rocks surrounding the Arpont schist, in which the geometry of D_3 folds and

shear-zones suggest substantial ESE-directed subhorizontal shear (Platt & Lister in review). In the Arpont area, the S–SE-vergent D_3 folds and crenulations are consistent with this. D_3 constitutes a back-thrusting event that is quite distinct in time and tectonic significance from the earlier deformational history. The cause of this event is not clear, but it is probably related to the Oligocene and younger deformations in the External Zones of the Alps.

CONCLUSIONS

The Arpont schist is a body of pre-Permian amphibolite-facies metamorphic rock that has been affected by a relatively early Alpine high-pressure metamorphic event. It now forms a fault-bounded thrust sheet or nappe that also includes some pre-Triassic sediments. The earliest deformation (D_1) recognizable in the field postdates the high-pressure peak, and was associated with nappe formation. D_1 and D_2 may have formed during a continuous tectonic event involving NW-directed subhorizontal shear. Metamorphic parageneses suggest decreasing pressure during this period, and hence uplift, which could have been caused either by erosion or by a tectonic process such as gravity spreading or regional horizontal extension. This was followed by an upper greenschist-facies static metamorphism possibly related to the late-Eocene Lepontine event in the Swiss Alps. SE-directed thrusting and folding (D_3) caused localized deformation and inverted the western margin of the nappe.

Acknowledgements—We are deeply indebted to Jacqueline Desmons for introducing us to the problems of the Arpont area, and for her continued interest and encouragement. We are grateful to Geoff Milnes, Frank Peel, Reinoud Vissers and Paul Williams for discussions, and to John Ramsay and Andy Siddans for helpful criticisms of the manuscript. Clare Pope, Andria Fowler and Richard Macavoy helped with draughting, typing and photography. Annie Bonati, gardienne of the Refuge de l'Arpont, is thanked for her kindness, during our days on the mountain.

REFERENCES

Bocquet (Desmons), J. 1971. Cartes de répartition de quelques minéraux du métamorphisme alpin dans les Alpes franco-italiennes. *Eclog. geol. Helv.* **64**, 71–103.

Bocquet (Desmons), J. 1974a. Études minéralogiques et pétrologiques sur les métamorphismes d'âge alpin dans les alpes françaises. Thèse d'Etat, Grenoble.

Bocquet (Desmons), J. 1974b. Le socle briançonnais de Vanoise (Savoie): arguments en faveur de son âge anté-alpin et son polymétamorphisme. *C. r. hebd. Séanc. Acad. Sci.*, Paris **178D**, 2601–2604.

Bocquet (Desmons), J., Delaloye, M., Hunziker, J. C., & Krummenacher, D. 1974. K–Ar and Rb–Sr dating of blue amphiboles, micas, and associated minerals from the western Alps. *Contr. Miner. Petrol.* **47**, 7–26.

BRGM 1979. *Carte géologique de la France à 1:250,000, feuille Annecy*. Bureau des Recherches Géologiques et Miniéres, Orleans.

Caby, R., Kienast, J-R., & Saliot, P. 1978. Structure, métamorphisme et modéle d'évolution tectonique des Alpes Occidentales. *Revue Géogre phys. Géol. dyn.* **20**, 307–322.

Compagnoni, R., Dal Piaz, G. V., Hunziker, J. C., Gosso, G., Lombardo, B., & Williams, P. F. 1976. The Sesnia–Lanzo Zone, a slice of continental crust with Alpine high-pressure low-temperature assemblages in the Western Italian Alps. In: *High Pressure–Low Temperature Metamorphism of the Oceanic and Continental Crust in the Western Alps*. Consiglio Nazionale Richerche, Torino, 123–176.

Debelmas, J. 1976. Deux coupes transversales des Alpes franco-italiennes. *Schweiz. miner. petrogr. Mitt.* **56**, 561–565.

Debelmas, J. 1974. *Géologie de France*, Doin, France.

Delaloye, M. & Desmons, J. 1976. K–Ar radiometric age determinations of white micas from the Piemont Zone, French–Italian Western Alps. *Contr. Miner. Petrol.* **57**, 297–303.

Desmons, J. 1977. Mineralogical and petrological investigations of Alpine metamorphism in the internal French Western Alps. *Am. J. Sci.* **277**, 1045–1066.

Ellenberger, F. 1958. Étude géologique du pays de Vanoise. *Mém. Carte géol. Fr.* **15**. Bureau de Recherches Géologiques et Miniéres. Orléans, France.

Ellenberger, F. 1960. Sur une paragénèse éphémère à lawsonite et glaucophane dans le métamorphisme alpin en Haute-Maurienne (Savoie) *Bull. Soc. géol. Fr.* **9**, 190–194.

Ellenberger, F. 1966. Le Permien du Pays de Vanoise. In: *Atti del Symposium sul Verrucano Pisa*, settembre 1965. Soc. Toscana di Scienze Naturali, Pisa, 170–211.

England, P. C. 1978. Some thermal considerations of the Alpine metamorphism—past, present, and future. *Tectonophysics* **46**, 21–40.

Ernst, W. G. 1973. Interpretative synthesis of metamorphism in the Alps. *Bull. geol. Soc. Am.* **84**, 2053–2078.

Frey, M., Hunziker, J. C., Frank, W., Bocquet, J., Dal Piaz, D. V., Jäger, E. & Niggli, E. 1974. Alpine metamorphism of the Alps: a review. *Schweiz. Miner. Petrogr. Mitt.* **54**, 247–289.

Frey, M., Hunziker, J. C., O'Neil, J. R. & Schwander, H. W. 1976. Equilibrium–disequilibrium relations in the Monte Rosa granite, western Alps: petrological, Rb–Sr and stable isotope data. *Contr. Miner. Petrol.* **55**, 147–179.

Frisch, W. 1979. Tectonic progradation and plate tectonic evolution of the Alps. *Tectonophysics.* **60**, 121–139.

Goffé, B. 1975. Étude structurale et pétrographique du versant occidental du massif paléozoïque de Chasseforêt (Vanoise méridionale). Thèse 3me Cycle, Univ. Paris-Sud.

Goffé, B. 1977. Succession de subfacies métamorphiques en Vanoise méridionale (Savoie). *Contr. Miner Petrol.* **62**, 23–42.

Goffé, B. 1982. Definition du faciès à Fe,Mg-carpholite–chloritoïde, un marquer du métamorphisme de HP-BT dans les métasediments alumineux. Mem. Sc. Terre Univ. Curie, Paris.

Homewood, P., Gosso, G., Escher, A., & Milnes, A. G. 1979. Cretaceous and Tertiary evolution along the Besançon–Biella traverse (Western Alps). *Eclog. geol. Helv.* **73**, 635–649.

Liou, J. G. 1971. P–T stabilities of laumonite, wairakite, lawsonite, and related minerals in the system $CaAl_2Si_2O_8$–SiO_2–H_2O. *J. Petrology* **12**, 379–411.

Milnes, A. G. 1978. Structural zones and continental collision, Central Alps. *Tectonophysics* **47**, 369–392.

Milnes, A. G., Greller, M. & Müller, R. 1981. Sequence and style of major post-nappe structures, Simplon–Pennine Alps. *J. Struct. Geol.* **3**, 411–420.

Newton, R. C. & Kennedy, G. C. 1963. Some equilibrium reactions in the join $CaAl_2Si_2O_8$–H_2O. *J. geophys. Res.* **68**, 2967–2984.

Newton, R. C. & Smith, J. V. 1967. Investigations concerning the breakdown of albite at depth in the earth. *J. Geol.* **75**, 268–286.

Platt, J. P. & Lister, G. S. 1978. Déformation, métamorphisme et mécanismes d'écoulement dans le massif de la Vanoise, Alpes penniques françaises. *C. r. hebd. Séanc. Acad. Sci.* **287D**, 895–898.

Platt, J. P. & Lister, G. S. (in review). Structural evolution of a nappe complex, southern Vanoise massif, French Pennine Alps. *J. Struct. Geol.*

Platt, J. P. & Vissers, R. L. M. 1980. Extensional structures in anisotropic rocks. *J. Struct. Geol.* **2**, 397–410.

Raoult, J. F. 1980. Interprétation nouvelle de la Vanoise (zone briançonnaise, Alpes françaises). *Revue Géog. phys. Géol. dyn.* **22**, 303–312.

Saliot, P. 1979. La jadéite dans les Alpes françaises. *Bull. Mineral.* **102**, 391–401.

Trümpy, R. 1975. Penninic-Austroalpine boundary in the Swiss Alps: a presumed former continental margin and its problems. *Am. J. Sci.* **275A**, 209–238.

White, S. H., Burrows, S. E., Carreras, J., Shaw, N. D. & Humphreys, F. J. 1980. On mylonites in ductile shear zones. *J. Struct. Geol.* **2**, 175–187.

Winkler, H. G. F. 1974. *Petrogenesis of Metamorphic Rocks*. 3rd Edition. Springer, Berlin.